Electronic Journal of Biotechnology 79 (2026) 100701

Contents lists available at ScienceDirect

Electronic Journal of Biotechnology

journal homepage: www.elsevier.com/locate/ejbt

Research article

Anoikis- and m6A-related lncRNA analysis to identify prognostic indicators in liver hepatocellular carcinoma ☆

Pan Yu [a], Shuaiyang Jing [b], Sarinder Kaur Dhillon [a,*]

[a] Data Science & Bioinformatics Laboratory, Institute of Biological Sciences, Faculty of Science, Universiti Malaya, Kuala Lumpur, Malaysia
[b] Department of Pharmacology, School of Medicine, Southern University of Science and Technology, Shenzhen, Guangdong, China

GRAPHICAL ABSTRACT

Anoikis and m6A related lncRNAs analysis to identify prognostic indicators in liver hepatocellular carcinoma.

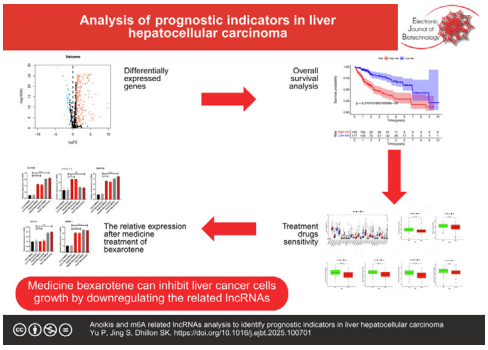

ARTICLE INFO

Article history:
Received 22 April 2025
Accepted 26 August 2025
Available online 5 December 2025

Keywords:
Anoikis
Chemotherapy drugs
Liver cancer
Liver hepatocellular carcinoma
lncRNAs
m6A
N6-methyladenosine
Prognostic indicators

ABSTRACT

Background: In cancer, the process of anoikis is intimately associated with the emergence and progression. N6-methyladenosine modification and m6A modification play an important role in regulating long non-coding RNAs. The liver hepatocellular carcinoma patients' data, including clinical and prognostic data, were obtained via The Cancer Genome Atlas database. The univariate, multivariate Cox and Least Absolute Selection Operator (LASSO) regression were performed to gain anoikis- and m6A-related lncRNAs. The Kaplan-Meier method was employed to assess the overall survival rate for groups of high- and low risks.

Results: A signature comprising six anoikis- and m6A-related lncRNAs was constructed: AL117336.3, LINC01138, Z83851.1, NRAV, CASC19 and AC009283.1. The clinicopathological variables, the anoikis- and m6A-related lncRNA signature demonstrated superior diagnostic efficacy, with an area under the receiver operating characteristic curve of 0.810. In the high-risk group, the overall survival was shown to be inferior to that of in group of low risk, while patients were classified by distinct clinicopathological variables. The ssGSEA and CIBERSORT immune analysis demonstrated that the predictive signature was significantly associated with liver cancer patients' immune status. The chemotherapy drugs ATRA, AUY922, bexarotene, gemcitabine, mitomycin-C, and PHA have been found to have greater sensitivity

☆ Audio abstract available in Supplementary material.

Peer review under responsibility of Pontificia Universidad Católica de Valparaíso.

* Corresponding author.
E-mail address: sarinder@um.edu.my (S.K. Dhillon).

https://doi.org/10.1016/j.ejbt.2025.100701

in treating high-risk patients. qRT-PCR showed that Z83851.1, NRAV and CASC19 lncRNAs were associated with poor prognosis and were high-risk factors. AC009283.1 lncRNA may have anti-cancer properties.

Conclusions: The predictive signature is capable of independently predicting the prognosis of liver cancer patients for understanding the mechanisms of anoikis- and m6A-related lncRNAs in liver hepatocellular carcinoma and offering clinical guidance to patients with liver cancer.

How to cite: Yu P, Jing S, Dhillon SK. Anoikis and m6A related lncRNAs analysis to identify prognostic indicators in liver hepatocellular carcinoma. Electron J Biotechnol 2026;79. https://doi.org/10.1016/j.ejbt.2025.100701.

1. Introduction

Among the most common cancers, hepatocellular carcinoma (HCC) was ranked sixth, being the third most prevalent cause of mortalities associated to cancers worldwide and having an overall survival rate at five years below 12% [1]. The HCC patients with good liver function do not experience cirrhosis; the hepatic resection (RES) can be the traditional treatment [2]. However, despite a nearly 70% five-year survival rate, recurrence rates after surgery are high [3]. For patients with multiple-site tumor recurrence or underlying liver cirrhosis, repeated hepatectomies are often not appropriate [2]. Significant progress has been made in cancer immunotherapies, especially for the blockade of the PD-1 and PD-L1 pathways, which has been proven to enhance hepatocellular carcinoma patients' five-year survival rate [4]. Nevertheless, the precise molecular mechanisms underlying hepatocellular carcinoma remain poorly understood, and PD-1/ PD-L1 blockade medication therapy efficacy was limited, with just 20–30% of patients deriving benefit [5]. So, it is of paramount importance to identify additional prognostic markers to guide the stratification of hepatocellular carcinoma patients based on risk and personalize therapy to better survival [6].

Normal cells detach from native extracellular matrix (ECM) and undergo programmed cell death, referred to name anoikis [7]. Physiologically, it effectively eliminates dislodged cells and inhibits the adhesion of detached cells to other tissues, thereby exerting a pivotal influence on tissue homeostasis and development [8]. However, it is also a participant in pathological processes and has a strong correlation between this factor and human cancer development [9]. A vital element of cancer metastasis is how cells in the circulatory system survive in distant organs without native ECM contacts, necessitating the capacity to resist anoikis [10]. In stomach, lung and breast cancers, the deregulation to resist anoikis has been documented [11]. It has been demonstrated that overexpression of NADPH oxidase 4 is related to the increasing generation' reactive oxygen species as well as upregulated expression of Epidermal Growth Factor Receptor, which together led to gastric cancer anoikis resistance and enhanced its metastatic potential [12,13]. Furthermore, anoikis resistance influences treatment resistance. Even though in the progression of hepatocellular carcinoma, anoikis is an essential factor, its prognostic value in HCC has not been subjected to a comprehensive evaluation.

In higher eukaryotic cells, the most prevalent, widespread, and well-preserved internal cotranscriptional modification is N6-methyladenosine (m6A). The m6A modification is subject to modification via m6A methyltransferases and removal by demethylases or recognized via m6A binding proteins [14]. Furthermore, they can also be the dynamic deposition of this mark for mRNAs and other forms of nuclear RNA [15]. vir like m6A methyltransferase associated (VIRMA), induces N6-methyladenosine-dependent post-transcriptional modification of GATA-binding protein 3 (GATA3) and is involved in the progression of liver cancer [16]. WT1-associated protein (WTAP), via m6A-HuR-dependent epigenetic silencing of ETS proto-oncogene 1(ETS1), has been shown to be a promoter of hepatocellular carcinoma progression [17]. alkB homolog 5(ALKBH5) was found to be overexpressed in several cancer types, promoting cancer emergence and development, including regulating immune cell infiltration of tumors. In some tumors, ALKBH5 has been suggested as a potential prognostic and immunotherapeutic biomarker [18]. In hepatocellular carcinoma, long non-coding RNA miR-503HG is the prognostic indicator of tumor metabolism through the modulation of the HNRNPA2B1/ NF-κB pathway [19].

RNA molecules cannot encode proteins, and under two hundred nucleotides are classified as long noncoding RNAs (lncRNAs) [20]. These molecules significantly influence gene expression regulation, transcripting genes, translating proteins, modifying proteins and other cellular mechanisms [21]. LncRNAs can affect cancer by modulating cellular signaling pathways, contributing to tumorigenesis, metastasis, prognosis, and diagnosis [22]. The long noncoding RNAs' expression profile has been shown to act being a prognostic biomarker in cancers, improving patient survival rate [23]. Noncoding RNAs are vital in tumor proliferation and migration, which may be regarded as a prospective biomarker [24]. Hence, studying the lncRNAs' expression may help assess the hepatocellular carcinoma prognosis.

We developed a predictive signature utilizing anoikis-associated long noncoding RNAs in this investigation. The study aimed to evaluate the biomarker's utility in the prediction of prognosis, diagnostics, chemo-response and immune infiltration of tumor for hepatocellular carcinoma patients and conduct internal validation. The gene sequence enrichment analysis was also used to find any underlying mechanisms.

2. Materials and methods

2.1. Datasets and patients

As shown in Fig. 1, we downloaded related clinical and prognostic data via The Cancer Genome Atlas (https://www.cancer.gov/ccg/research/genome-sequencing/tcga). RNA-seq data are standardized according to the transcripts per million mapped reads' fragments per kilobase (FPKM). A total of 377 patients containing lncRNA expression levels as well as survival time data were enrolled in this study. Also, 794 anoikis-related genes and 350 m6A-related genes were sourced from the Gene Cards database (https://www.genecards.org/) [25].

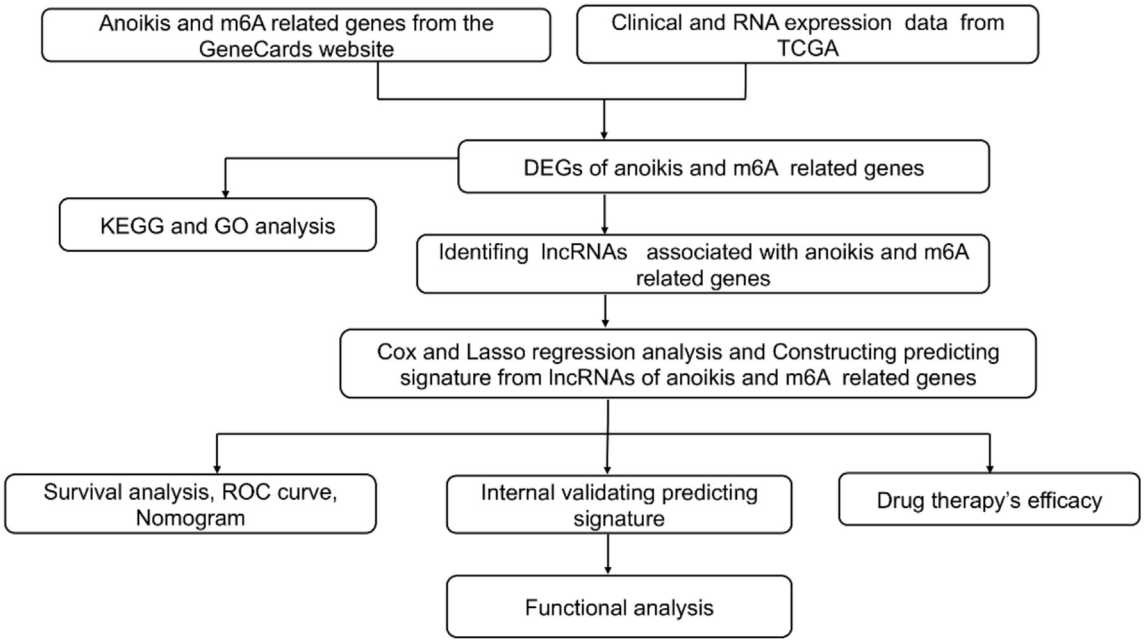

Fig. 1. The research flowchart. TCGA for The Cancer Genome Atlas, DEGs for differentially expressed genes, KEGG for Kyoto Encyclopedia of Genes and Genomes, GO for Gene Ontology, lncRNAs for long noncoding RNAs, and ROC for receiver operating characteristic.

2.2. Anoikis- and m6A-related differentially expressed genes' functional enrichment analysis

For acquiring of anoikis- and m6A-related differentially expressed genes, we set the screening criteria of value of an adj. p-value less than 0.01 and a value of |log FC| greater than 1. The packages "clusterProfiler" and "ggplot2" were utilized of Gene Ontology and Kyoto Encyclopedia of Genes for Genomes analyses.

2.3. Establishing a predicting signature for anoikis- and m6A-related lncRNAs

The limma package was applied to differentially expressed genes. With the screening criteria $p < 0.001$ and $|R^2| > 0.4$, we obtained 286 lncRNAs associated with anoikis and m6A. In order to recognize long noncoding RNAs that were related to hepatocellular carcinoma patients' prognosis, initially, we conducted univariate and multivariate Cox regression analysis and subsequently Least Absolute Shrinkage and Selection Operator (LASSO) regression analysis (minimum error or 1-SE rule via 10-fold cross-validation). The formula employed for the calculation was [24]:

$$\beta : risk\,code = \sum_{i=1}^{n} \beta i * (expression\,of\,mRNAi)$$

2.4. Constructing nomogram

To predict survival rates at one-, three- and five-year intervals, a nomogram was developed. Furthermore, a calibration curve was employed for assessing the correlation between predictive and observed survival rates.

2.5. Anoikis- and m6A-related lncRNAs predicting signature' functional enrichment analysis

The patients were sorted into groups of low risk and high risk via their risk score's median value. For identifying the pathway genes that exhibited significant enrichment, we employed Gene Sequence Enrichment Analysis [26]. The Gene Sequence Enrichment Analysis has been performed with 4.1.0 version (https://www.gsea-msigdb.org/gsea/index.jsp). In order to ascertain statistical significance, a value of less than 0.25 was set to be the false discovery rate, while the p-value was set at a value of less than 0.05. Additionally, the package of GSVA was used for single-sample Gene Set Enrichment Analysis (ssGSEA). Thirteen immune-related pathways' activities, as well as sixteen immune cells' infiltration scores, were computed [27].

Immune infiltration analysis was performed using CIBERSORT.22 Immune cells including macrophages M2, plasma cells, neutrophils, mast cells activated, T cells CD8, macrophages M1, T cells gamma delta, B cells memory, monocytes, B cells naive, T cells follicular helper, NK cells activated, T cells CD4 memory activated, T cells CD4 naive, NK cells resting, T cells regulatory (Tregs), dendritic cells activated, eosinophils, macrophages M0, T cells CD4 memory resting and mast cells resting. The results were analyzed by programmatically filtering the results according to the cut-off criterion of adjusting the p-value less than 0.05 and using the barplot, corrplot and ggplot2 packages in R version 4.1.0 for visualization of each sample. The corrplot package calculates the relationship between the gene expression matrix and the immune cells [28].

2.6. Predicting signature for predicting clinical treatment response role

Genes for immune checkpoints were obtained from the literature, including 47 immune checkpoint genes. Analysis of immune checkpoints was performed using the R software packages limma, reshape2, ggplot2, ggpubr and beeswarm to extract significantly different genes, and high- and low-risk samples were analyzed for differences in immune checkpoint content and filtered according to the criterion of $p < 0.05$ [29,30,31]. The FPKM data were transformed into transcripts per million (TPM), and the data were normalized log2(TPM + 1) while retaining samples with recorded clinical information. We predicted the chemotherapy response

for each sample based on the largest publicly available pharmacogenomics database (Genomics of Drug Sensitivity in Cancer https://www.cancerrxgene.org/). The prediction process was implemented by the R package pRRophetic, in which the half-maximal inhibitory concentration (IC50) of the samples was estimated by ridge regression, all parameters were set at default values, the batch effect of combat and the tissue type of all were used, and the replicate gene expression was summarized as the mean value [32,33].

2.7. Validation of lncRNAs in several associated cell lines

Validation using associated cell lines was done to confirm the expression of the 6 lncRNAs between normal liver and liver cancer cell lines. The LX-2 human hepatic stellate cell lines have so far been used as a control group. The experimental groups were HepG2 and HuH7 liver cancer cell lines. LX-2 and Huh7 were grown in Gibco DMEM medium (with streptomycin and 10% fetal calf serum, 1% penicillin). RNA was extracted using Vazyme's Super FastPure Cell RNA Isolation Kit RC102-01. The reagent for the reverse transcription system (HiScript IV RT SuperMix for qPCR (+gDNA wiper) R423-01 from Vazyme) was used for cDNA extraction. Quantitative real-time PCR was performed (PCR Taq Pro Universal SYBR qPCR Master Mix Q712-02/03 Vazyme) and 10 microM primers on QuantStudio 7 Flex Life Technologies Holdings Pte Ltd. The relative expression values have been normalized to the level of the reference gene (GADPH). Table S1 contains the primer pairs.

2.8. Statistical analysis

We conducted the statistical analyses using R (version 3.6.3). We investigated the connection between anoikis-associated long noncoding RNAs and overall survival. Univariate and multivariate Cox regression analyses were applied to find the anoikis-related lncRNAs that could be used to develop a predictive signature. The log-rank test and the Kaplan-Meier method were used to contrast overall survival for groups of high risk and low risk. ROC curves were constructed, and the survivalROC package was used to calculate AUC values. The single-sample Gene Set Enrichment Analysis was applied by the package of GSVA.

3. Results

3.1. Enrichment analysis for anoikis- and m6A-related genes

By differentially expressed genes, we found 286 anoikis- and m6A-related genes, comprising 258 upregulating genes and 28 downregulating genes (Fig. 2A). KEGG pathway analyses showed anoikis- and m6A-related DEGs are enriched in the following genes: MAPK signaling pathway, Focal adhesion, signaling pathway of PI3K-Akt, infection of Human papillomavirus, AGE–RAGE signaling pathway as the top five upregulated DEGs, while the Cell cycle, Melanoma and p53 signaling pathway were downregulated (Fig. 2B). For biological processes, GO analysis indicated that difference was focused on negative regulating mitotic cell cycle, the cell aging, negative regulating cell cycle process, etc. As for cellular components classification, the genes of differentially expressed were mainly enriched in nuclear chromatin, focal adhesion, heterochromatin, etc. As for the molecular function, the gene's difference was mainly shown in serine/threonine kinase activity, transcriptional corepressor activities, and RNA polymerase II transcription factor binding (Fig. 2C).

3.2. Related lncRNAs predicting signature

As Table S2 shows, 953 anoikis- and m6A-related long noncoding RNAs were identified. Univariable Cox regression analysis shown 103 lncRNAs related to prognosis in HCC patients. Six anoikis- and m6A-related long noncoding RNAs were mostly related to survival in a LASSO regression hazards model (AL117336.3, LINC01138, Z83851.1, NRAV, CASC19, AC009283.1). Fig. 3A illustrates six anoikis- and m6A-related long noncoding RNAs' expression levels in the patients. Furthermore, the long noncoding RNAs were visualized with the Cytoscape software and the ggplot2 R package. As illustrated in Fig. 3B, LINC01138 and NRAV assume pivotal roles in the lncRNA-mRNA co-expression network ($|R^2|$ greater than 0.4, p less than 0.001).

3.3. Predicting the signature and prognosis of HCC patients' correlation

Overall survival time for the group of high risk was mostly shorter compared to that of the group of low risk (shown in

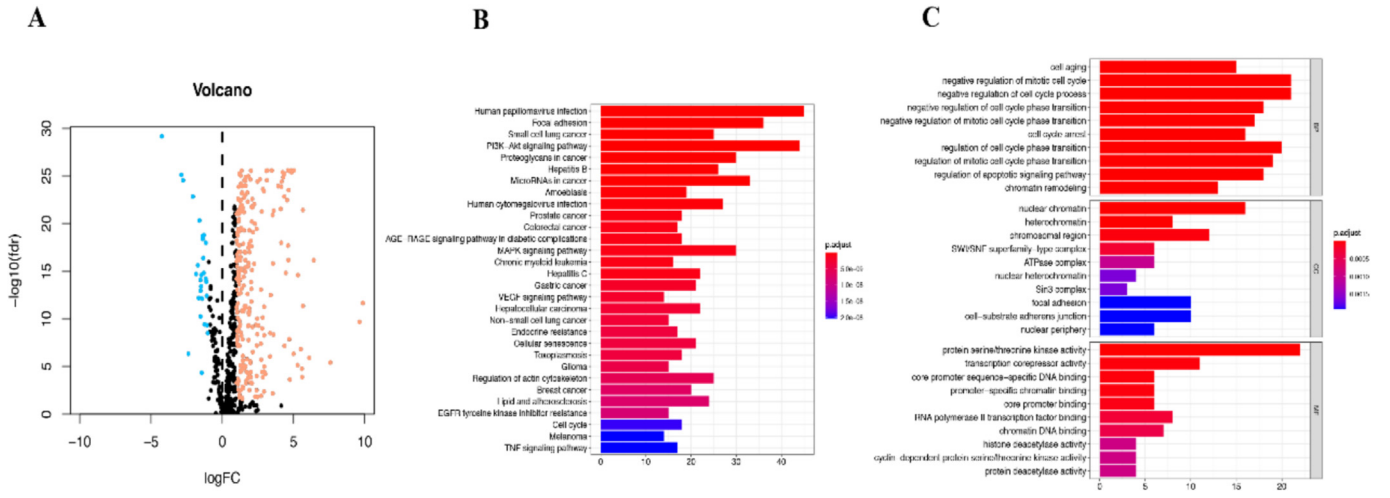

Fig. 2. Tissues of cancer and adjacent for GO and KEGG analyzing anoikis- and m6A-related DEGs. (A) 286 DEGs volcano plot in HCC. Blue, red dots represent downregulated and upregulated genes. (B) The DEGs of KEGG analysis. (C) The DEGs of GO analysis. (FC for fold change; fdr for false discovery rate; BP for biological process; CC for cellular components; MF for molecular function). (For interpretation of the references to color in this figure legend, the reader is referred to the web version of this article.)

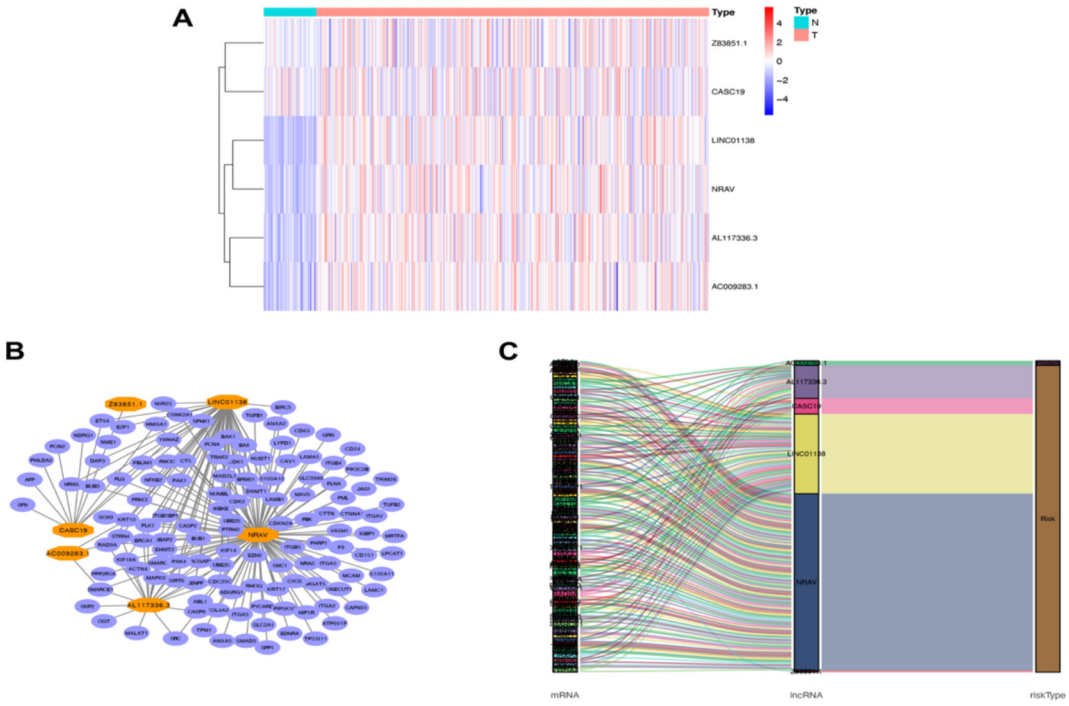

Fig. 3. Expression levels of predicting Signature in the six anoikis-, m6A-related lncRNAs and lncRNA-mRNA network. (A) The six lncRNAs expressed in HCC compared to normal tissues. (B) Prognostic lncRNA co-expression network. Orange Rhombus represents lncRNAs, and blue Ellipse shows mRNAs. (C) Sankey diagram for prognostic the lncRNAs. N, typical; T for tumor. (For interpretation of the references to color in this figure legend, the reader is referred to the web version of this article.)

Fig. 4A, p = 6.2191e-10). Five-year survival rates for the groups of high risk and low risk were 26.3% and 64.5%, respectively. Fig. 4B illustrates risk scores for groups of high risk and low risk. With risk score enhanced, patient deaths were also enhanced (Fig. 4C). The univariate cox regression analysis demonstrated that age, stage as well as risk score were considerably related by patients' overall survival (Fig. 4D). The multivariate cox regression analysis results indicated that risk score and age were independent predictors with overall survival within patients (Fig. 4E). The AUCs of one-, three-, and five-year survival were 0.78, 0.743 and 0.801 accordingly, which shown model demonstrating reliable predictive performance (Fig. 4F). The risk score' area under the curve was 0.810, which demonstrated a superior predictive capacity for HCC patients compared to clinicopathological variables (Fig. 4G). The distinctions in clinicopathological variables for groups of high risk and low risk were analyzed. N stage ($p < 0.05$), M stage ($p < 0.05$), stage ($p < 0.01$) and status ($p < 0.001$) in these two groups shown significant differences, which means the high and low groups do have statistical significance (Fig. 5).

3.4. Model line diagrams and calibration charts

A nomogram was constructed, incorporating clinicopathological variables as well as the risk score, for predicting the one-, three-, and five-year prognosis of patients of liver hepatocellular carcinoma (Fig. 6A). The calibration curves demonstrated high consistency for actual OS rates as well as predicted survival rates at one-, three-, and five-year intervals (Fig. 6B–D).

3.5. Predictive signature and prognosing HCC patients in different clinicopathological variables relationship

The aim was to find the relation between the predicting signature and the HCC patients' prognosis classified by various clinicopathological variables. The HCC patients were sorted into different groups via age, gender, grade, T-stage and N-stage. The patients' median overall survival in groups of high-risk was considerably shorter than that of patients in group of low risk (Fig. 7).

As the Fig. 8 shown, AC009283.1, AL117336.3, CASC19, LINC01138, and NRAV have a significant difference in high and low groups. (p value 0.007321729, 0.000156933, 0.004522616, 0.000497891 and 2.71E-08, respectively).

3.6. Internal validation of predictive signature

In the two cohorts, as Table 1 shows a comparison of patients' demographic characteristics. With findings observed in the overall dataset, in Fig. 9A, in the first internal cohort for the group of high-risk, the OS rate was inferior to that of patients in the group of low-risk (p = 7.8379e-07). Fig. 9B shows a poorer prognosis for the group of high risk than for the group of low risk within the second internal cohort (p = 0.000266). ROC curves demonstrated favorable predictive performance for two cohorts. AUCs were 0.833, 0.722 and 0.817 for one-, three- and five-year survival, for first internal cohort (Fig. 9C). Fig. 9D shows that the AUCs for the second internal cohort at one, three, and five years were 0.711, 0.773, and 0.805.

3.7. Gene enrichment analysis

Our findings demonstrated that the group of high-risk shows considerable enrichment within some biological pathways, like cell cycle signaling, purine metabolism signaling, pyrimidine metabolism signaling, RNA degradation and selenoamino acid metabolism (shown in Fig. S1, Table 2). This suggests that patients at high risk were linked to RNA and DNA metabolism pathways, indicating that patients at high risk are tightly associated with RNA and DNA metabolism-associated pathways.

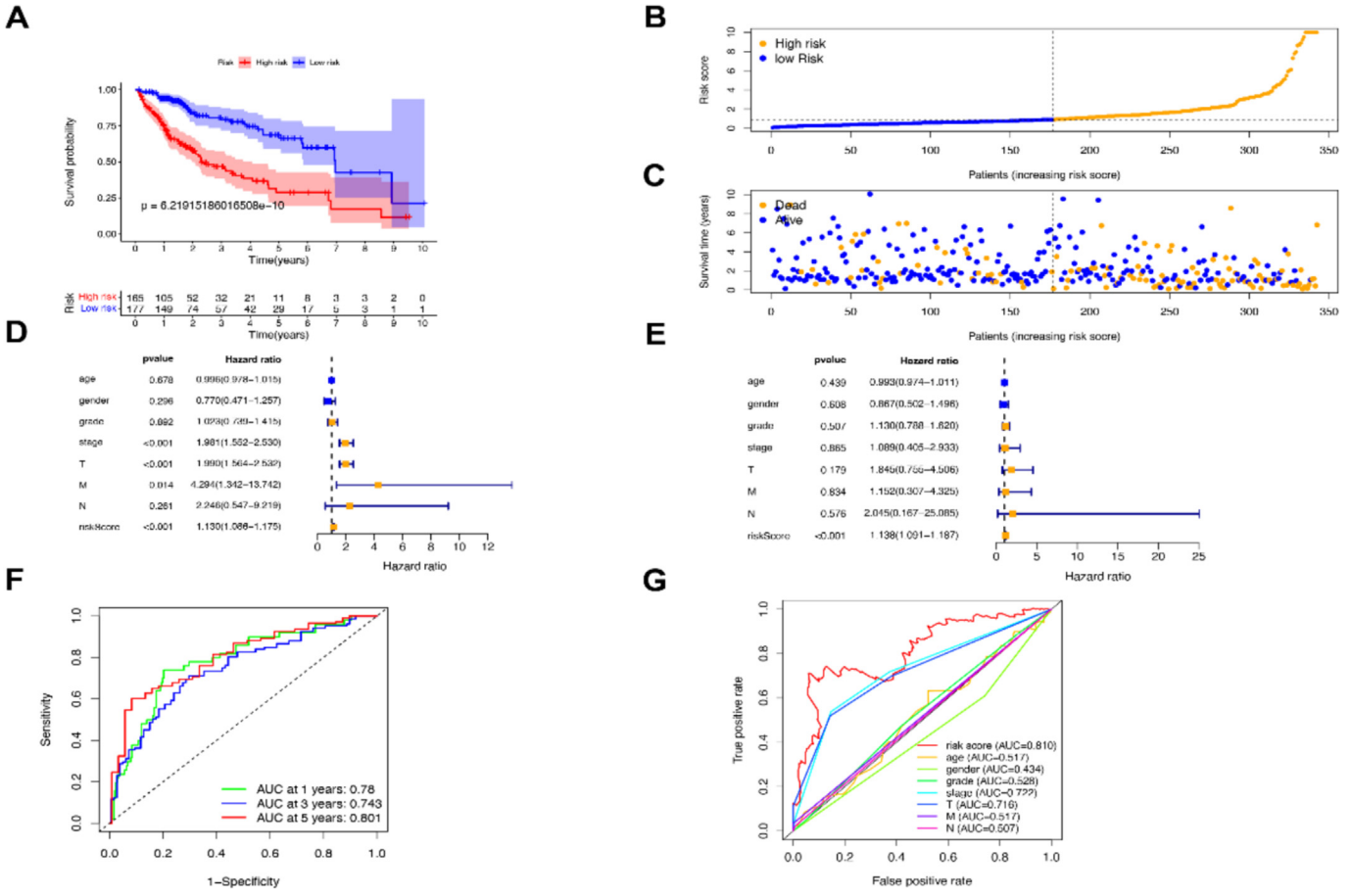

Fig. 4. Predicting Signature and the prognosis of HCC patients' correlation. (A) In groups of high- and low-risk Kaplan-Meier analyzing OS rate, (B) Among HCC patients of risk score distribution and (C) Number of patients alive and dead with different risk values. Blue and red represent the number of survivors and deaths. (D) Univariate cox regression analyzing forest plot and (E) Multivariate cox regression analyzing forest plot. (F) For predictive signature, AUC and ROC curve at one-year, three-year and five-year survival. (G) Clinicopathological variables and risk score' ROC curve. (For interpretation of the references to colour in this figure legend, the reader is referred to the web version of this article.)

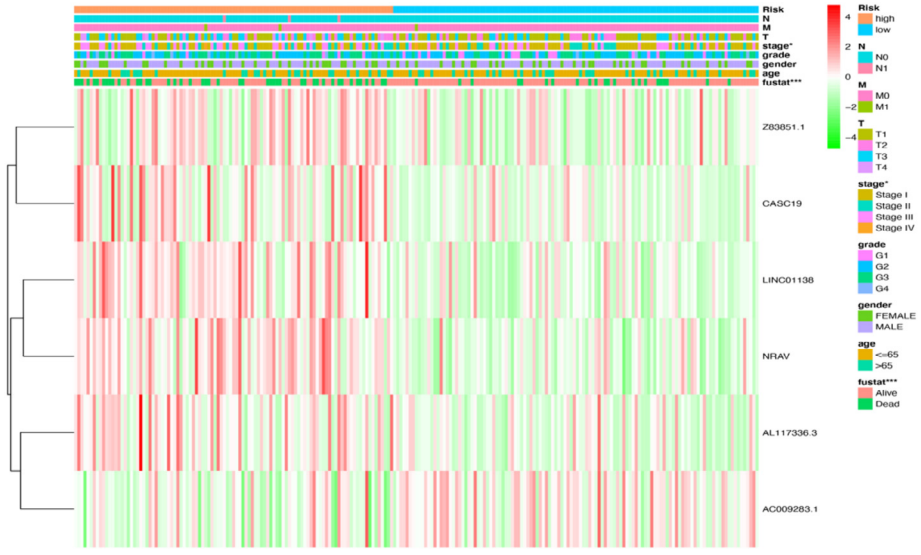

Fig. 5. In groups of high and low risks, the distribution heat map for six prognostic anoikis- and m6A-related long noncoding RNAs and clinicopathological variables.

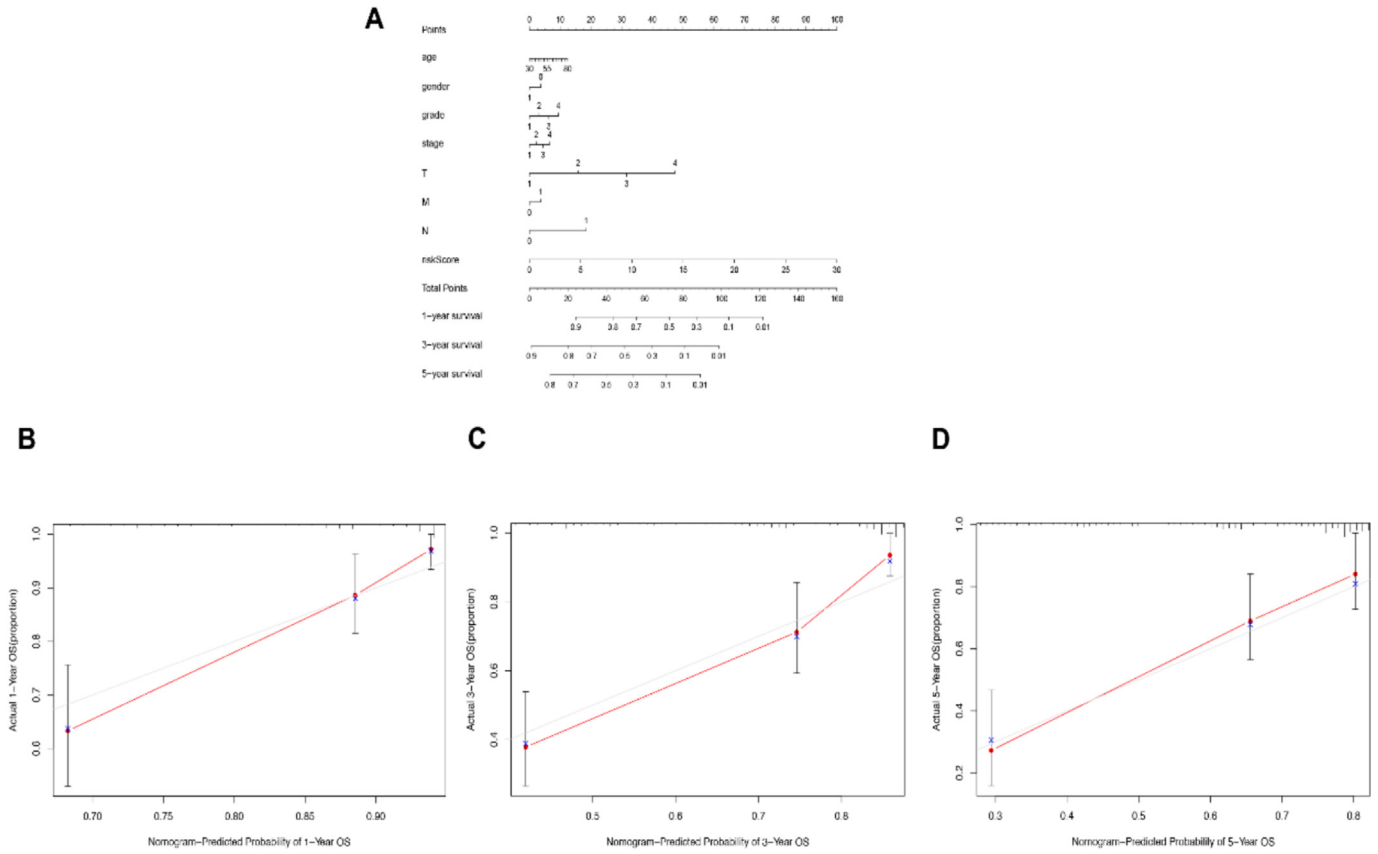

Fig. 6. Constructing and verifying nomogram. (A) The nomogram integrating clinicopathological variables and risk score predicts one-, three-, and five-year overall survival with HCC patients (B–D). The calibration curves are employed to ascertain the consistency in actual OS rates as well as predicted survival rates at one, three and five years.

3.8. Immune-related functions and immune cell infiltration

For levels of several immune cell populations in two groups, the findings showed considerable differences including activated dendritic cells, B cells, cells of $CD8^+$ T, immature-dendritic cells, neutrophils, natural killer, plasmacytoid-dendritic cells, cells of T helper, cells of T follicular helper, tumor-infiltrating lymphocytes and cells of T regulatory (Fig. 10A), and the immune function scores for chemokine receptor, checkpoint, inflammation-promoting, co-stimulation and co-inhibition of T cell, Type II IFN Response, as well as human leukocyte antigen, were found to be higher with group of high risk than that of low risk (Fig. 10B).

The CIBERSORT algorithm was used to explore the relevance between the risk score and tumor immune cell infiltration. Patients with HCC in the high-risk group had higher proportions of M0 macrophages ($p < 0.001$), M1 macrophages ($p = 0.006$), activated dendritic cells (p = 0.033), neutrophils ($p = 0.024$), whereas naive B cells ($p = 0.003$), CD8 T cells ($p = 0.042$), CD4 memory T cells ($p = 0.015$), follicular helper T cells ($p = 0.007$), activated NK cells ($p = 0.032$) and resting mast cells ($p = 0.004$) were negatively related to the risk score (Fig. 10C). This shows that our signature is not only a prognostic marker but also reflects the level of immune cell infiltration, as the abundant immune infiltration observed in the low-risk group partly reflects the reduction in malignancy and the effects of various treatments.

3.9. Differences between high-risk and low-risk groups in response to immunotherapy and chemotherapy therapy

Previous research has pointed to immune checkpoint blockade through epigenetic mechanisms as a promising strategy for the treatment of HCC, which may affect prognosis. We analyzed the expression levels of immune checkpoint genes between the high-risk and low-risk groups; in Fig. 11A, we identified 29 differentially expressed genes of immune checkpoint and its ligand between the high-risk and low-risk groups. CD276, LGALS9, CD80, TNFRSF9, LAIR1, TNFSF9, HAVCR2, CD86, TNFRSF4, HHLA2, VTCN1 were highly expressed in the high-risk groups. The findings indicated immunotherapy was associated with a greater chance of survival in patients at higher risk.

Analyzing the relationship between the predicting signature and conventional chemotherapy effectiveness in hepatocellular carcinoma, the IC50 of ATRA, AUY922, bexarotene, gemcitabine, mitomycin-C, and PHA.665752 were lower in the high-risk group (Fig. 11B–G). It is beneficial to study tailored treatment plans that are suited to patients in classifications of high and low risks.

3.10. Validation of predicted gene expression by qRT-PCR

Z83851.1, NRAV and CASC19 lncRNAs were upregulated in HepG2, HuH7 compared to the control group of LX-2 (Fig. 12), whereas the AC009283.1 was downregulated in the cells. AL117336.3 and LINC01138.3 showed no difference in the cell lines. The results of the analyses were further validated experimentally, and prognostic analyses showed that Z83851.1, NRAV and CASC19 lncRNAs were related to poor prognosis and were high-risk factors. AC009283.1 lncRNA may have anti-cancer properties.

3.11. Chemotherapy drug validation experiment

Drug experiments were selected based on the literature. The final concentration was one micromole. Cell lines were used.

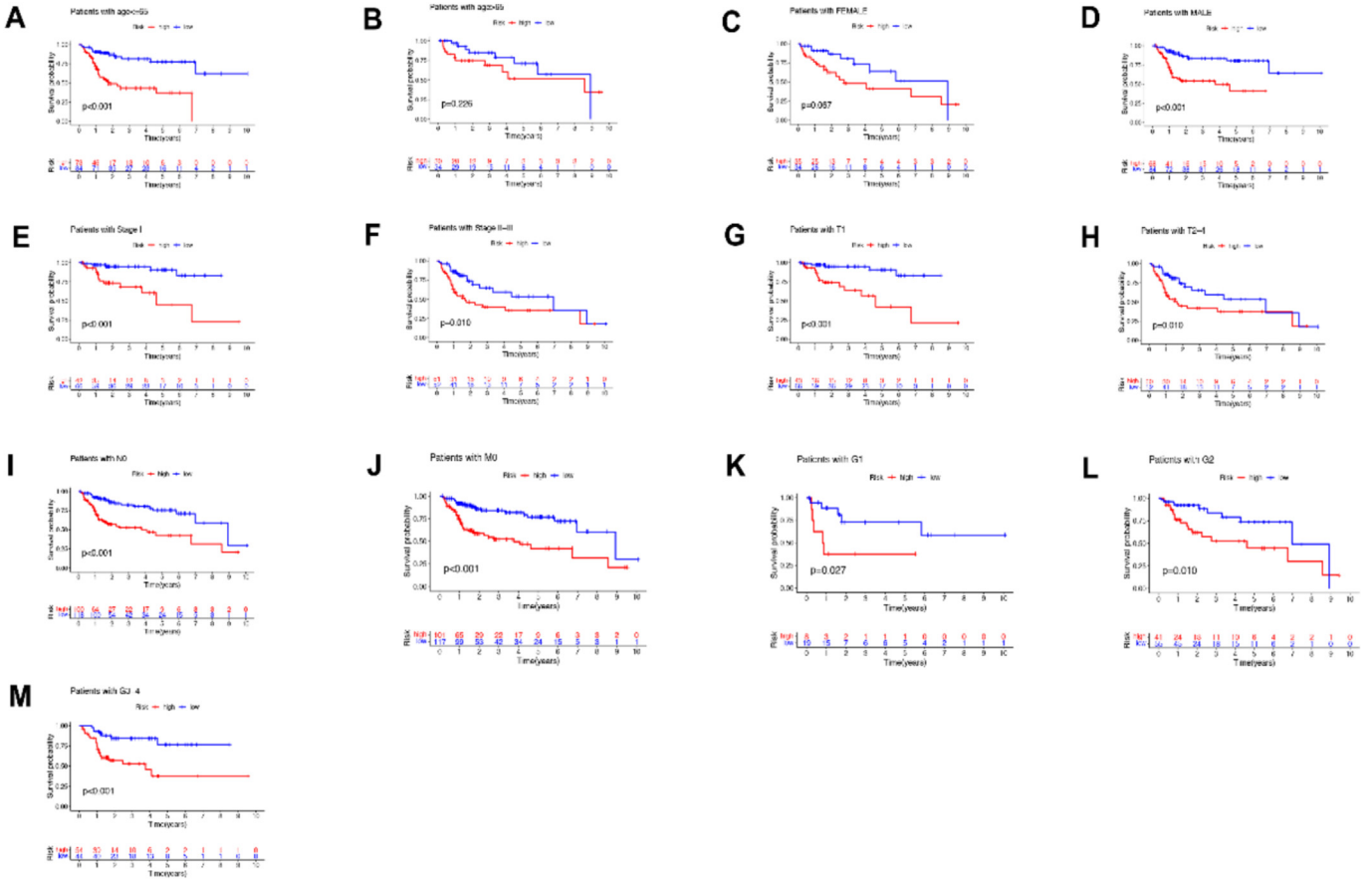

Fig. 7. Kaplan-Meier survival curves were constructed via clinicopathological variables in groups of high and low-risk. (A–B) For Age. (C–D) For Sex. (E–F) For Stage. (G–H) For T stage. (I–J) For M, N stage. (K–M) For G stage.

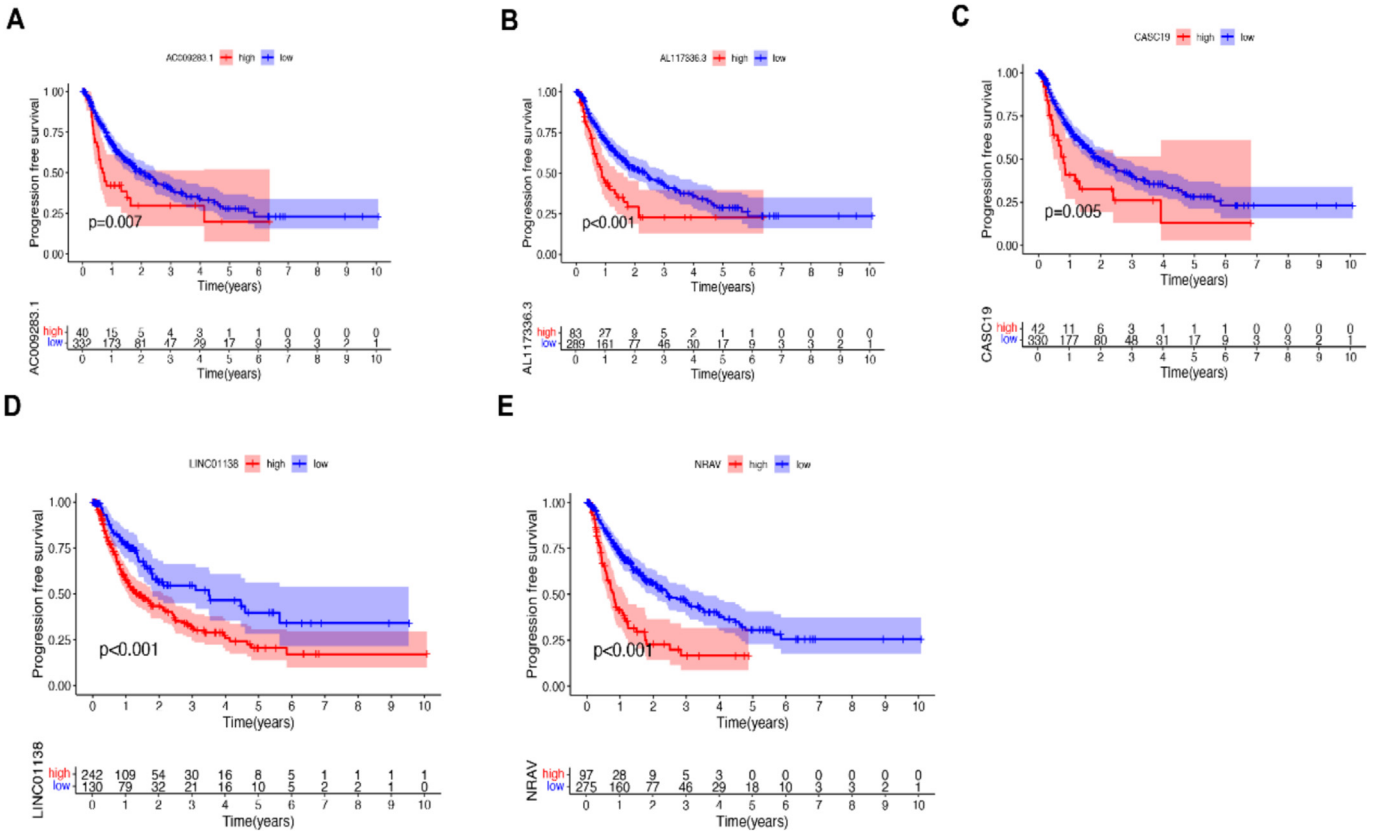

Fig. 8. Progression-free survival in groups of high and low risks for each gene. (A) AC009283.1 (B) AL117336.3 (C) CASC19 (D) LINC01138 (E) NRAV.

Table 1
Patients' clinical characteristics in different cohorts.

Variables	Entire	Validation	
	TCGA dataset (n = 342)	First cohort (n = 172)	Second cohort (n = 170)
Fustat (%)			
Alive	223 (65.20%)	112 (50.22%)	111 (49.78%)
Dead	119 (34.80%)	60 (50.42%)	59 (49.58%)
Age (%)			
≤65	216 (63.16%)	115 (53.24%)	101 (46.76%)
>65	126 (36.84%)	57 (45.24%)	69 (54.76%)
Gender (%)			
FEMALE	109 (31.87%)	53 (48.62%)	56 (51.38%)
MALE	233 (68.13%)	119 (51.07%)	114 (48.93%)
Stage (%)			
Stage I	161 (47.08%)	87 (54.04%)	74 (45.96%)
Stage II	77 (22.51%)	31 (40.26%)	46 (59.74%)
Stage III	80 (23.39%)	40 (50.00%)	40 (50.00%)
Stage IV + unknown	24 (7.01%)	14 (8.1%)	10 (5.89%)
T (%)			
T1	168 (49.12%)	90 (53.57%)	78 (46.43%)
T2	84 (24.56%)	35 (41.67%)	49 (58.33%)
T3	112 (50.68%)	51 (45.54%)	61 (54.46%)
T4 + unknown	74 (32.75%)	39 (52.70%)	35 (47.30%)
M (%)			
M0	244 (71.35%)	116 (47.54%)	128 (52.46%)
M1 + unknown	98 (28.65%)	56 (57.14%)	42 (42.86%)
N (%)			
N0	239 (69.88%)	113 (47.28%)	126 (52.72%)
N1 + NX + unknown	103 (30.12%)	59 (57.28%)	44 (42.72%)
G (%)			
G1	53 (15.50%)	34 (64.15%)	19 (35.85%)
G2	161 (47.08%)	80 (49.70%)	81 (50.31%)
G3-4	123 (35.96%)	55 (44.72%)	68 (55.28%)
Unknown	5 (1.50%)	3(60.00%)	2(40.00%)

Analysis was performed using quantitative Reverse Transcription Polymerase Chain Reaction (qRT-PCR).

As shown in Fig. 13, comparing with Fig. 12 results, the drug dose indeed have a specific effect in downregulating lncRNAs, CASC19, LINC01138, NRAV, and Z83851.1 expression, which has been downregulated, while AL117336.3 has been upregulated. However, finally, it has a certain inhibitory effect on liver cancer cells.

4. Discussion

The hepatocellular carcinoma was ranked sixth, being the third most prevalent cause of mortalities, of which the five-year overall survival rates are relatively low. The anoikis' role in cancer is complex and multifaceted, and further research is required to elucidate its mechanisms fully. Anoikis has been regarded as a critical element in cancer development and progression in a growing number of studies [7,34,35,36]. There is a dearth of research in the field of anoikis and prognostication of cancer, given the limited number of studies conducted in this area. However, recently research has commenced which predicts the prognosis of cancer patients by constructing anoikis-related long noncoding RNA predictive signatures [37,38,39,40]. There are a few reports on applying anoikis- and m6A-related lncRNAs predictive signatures to predict the HCC patients' prognosis [41]. The present study demonstrated the integration of anoikis with m6A-related lncRNAs, which is a novel approach in predicting HCC disease prognostication. This study initially identified 286 differentially expressed genes related to anoikis. Findings indicated that the X protein of hepatitis B virus has been demonstrated to inactivate the p53 gene by the p38/MAPK pathway, thereby inducing primary liver cancer [42]. It is shown that p53 can induce anoikis in cancer cells via activating the apoptotic program. The results indicated that anoikis-related genes may change the hepatocellular carcinoma progression by the p53 signaling pathway [43]. Nevertheless, in HCC, further

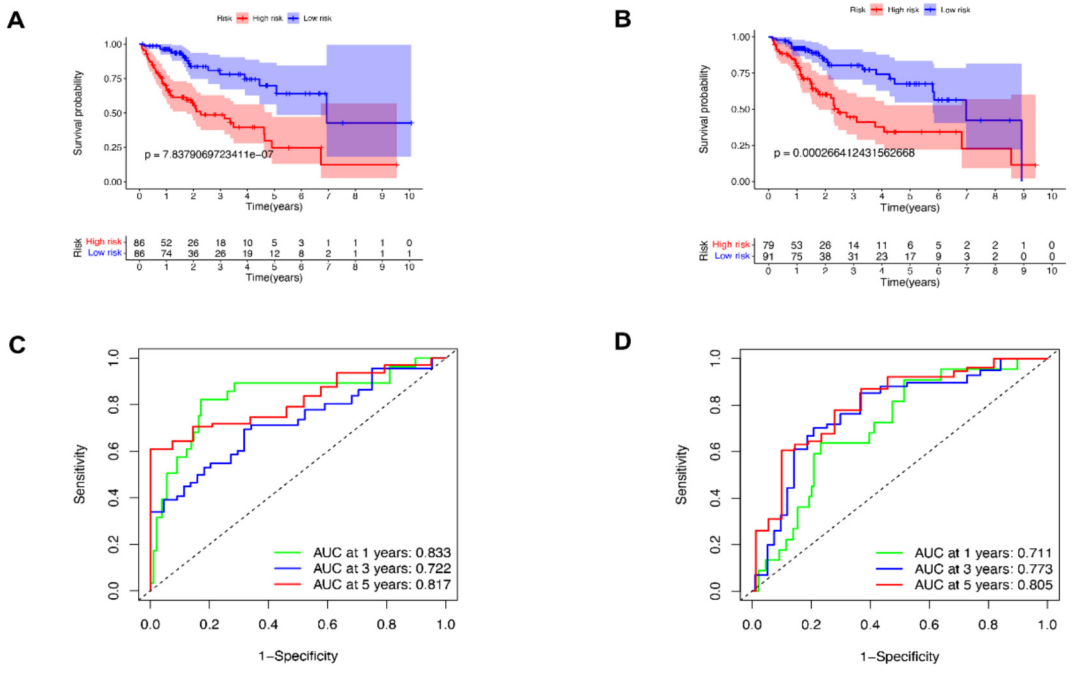

Fig. 9. In the whole TCGA dataset, the internal validation of the predicting signature for OS. (A) The first internal cohort 'Kaplan-Meier survival curve and (B) The second internal cohort Kaplan-Meier survival curve. (C) The first internal cohort's curve and AUCs at one-year, three-year and five-year survival. (D) The second internal cohort's curve and AUCs at one-year, three-year and five-year survival.

Table 2
Enriched gene sets for a group of high risk.

Gene set	ES	NES	NOM p-value	FDR q-value
pyrimidine metabolism signaling	0.675472	2.187865	0	0
RNA degradation	0.762306	2.154974	0	0
selenoamino acid metabolism	0.687936	2.123658	0	3.65E-04
purine metabolism signaling	0.582457	2.065042	0	0.001706
cell cycle signaling	0.717232	2.012248	0	0.007123

ES: enrichment score; NES: normalized enrichment score.

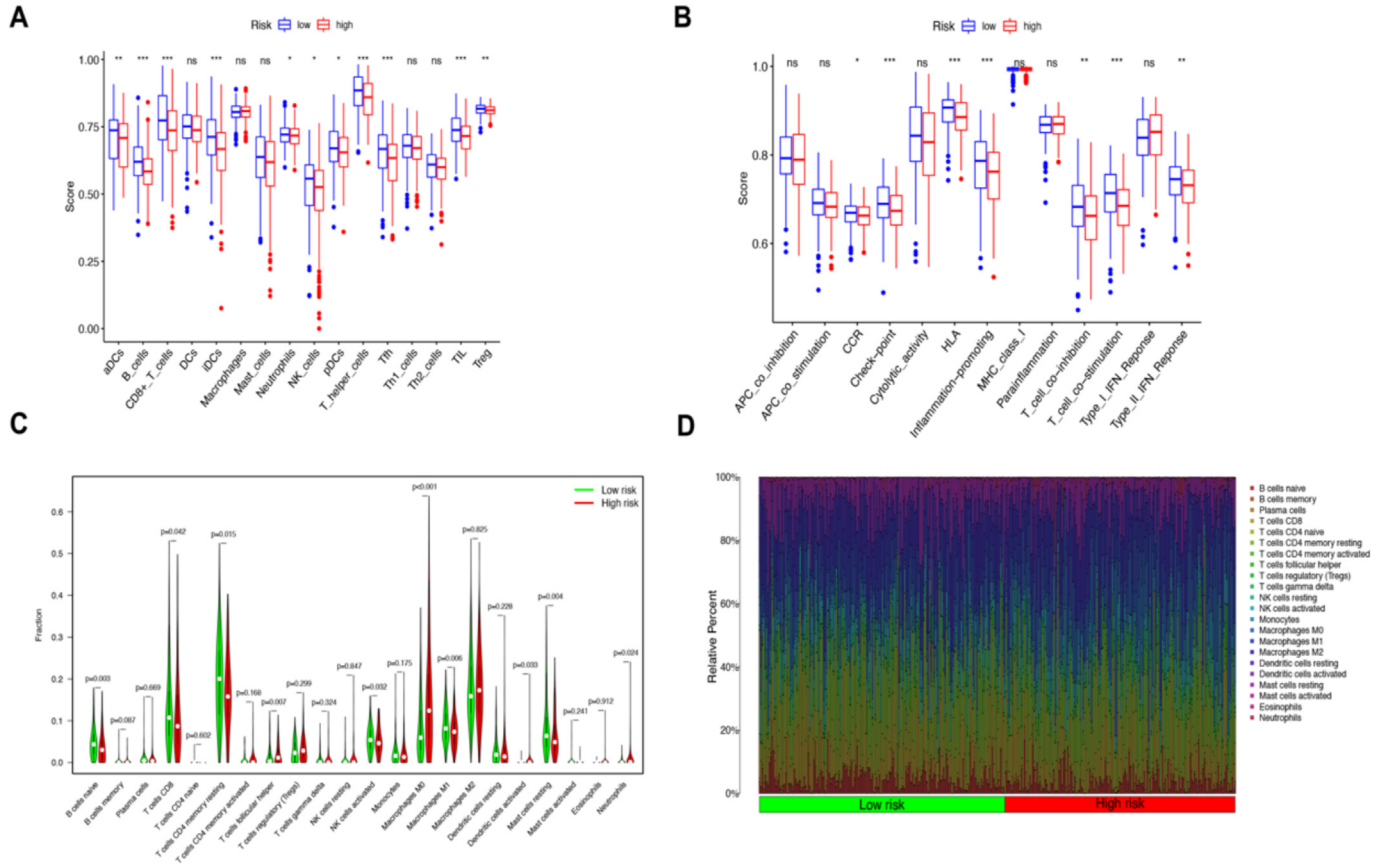

Fig. 10. The analysis of immune infiltrating cells and immune-related functions in high- and low-risk groups. (A) ssGSEA algorithm for the calculation of infiltration levels of 16 immune cells in two groups. (B) Analysis of immune-related function scores in two groups. (C) A violin plot of immune-infiltrating lymphocytes in two groups. (D) Bar chart showing the percentage of 22 types of TICs in HCC tumor samples. Column names of the graph were sample ID. $^{*}p < 0.05$; $^{**}p < 0.01$; $^{***}p < 0.001$; ns, non-significant.

experiments are to be completed to validate the workings of the anoikis-related genes.

Much evidence from research studies showed that long-noncoding RNAs were pivotal in hepatocellular carcinoma [44]. Furthermore, many investigations have shown that lncRNAs are instrumental with anoikis [45,46,47]. lncRNA of APOC1P1-3 specifically can bind to miRNA-188-3p and has been indicated to strengthen anoikis resistance within cells of breast cancer. This binding acts as a competitive inhibitor, effectively blocking the Bcl-2 inhibition [47]. A large-sized and rarely spliced lncRNAs named metastasis-associated lung adenocarcinoma transcript 1 (MALAT1), which are implicated within several gynecological cancers. MALAT1 overexpression has been found in ovarian, breast, cervical and endometrial cancers. This has been linked to the initiation of cancer progression, through the induction and promotion of alterations in the expression of multiple antiapoptotic genes associated with epithelial-to-mesenchymal transition [48,49]. The results demonstrated that 103 RNAs were related to the prognosis of hepatocellular carcinoma patients. In our study, six m6A- and anoikis-related long noncoding RNAs (AL117336.3, LINC01138, Z83851.1, NRAV, CASC19, AC009283.1) were identified in a predictive signature following LASSO regression analysis. CASC19 is related to the progression in colorectal cancer, advanced gastric cancer, non-small cell lung, and hepatocellular carcinoma [50,51,52,53,54,55]. A poorer prognosis was related to higher CASC19 expression. Furthermore, experiments indicated that CASC19 overexpression increased cell invasion, migration and proliferation, which was also confirmed by our work. Cell migration-inducing hyaluronidase 1 (CEMIP) and epithelial-mesenchymal transition markers were upregulated by CASC19 overexpression. MiR-140-5p bound directly to CASC19 and CEMIP. Overexpressed miR-140-5p reversed the effects of CASC19 on cell proliferation and tumor migration and inhibited CASC19-induced CEMIP expression. In non-small cell lung cancer, LncRNA CASC19 regulates miRNA-130b-3p and enhances proliferation, migration and invasion [50]. With ETS1 expression upregulated, CASC19, a long non-coding RNA, sequesters microRNA-532 and contributes to the oncogenic potential of clear cell renal cell carcinoma [56].

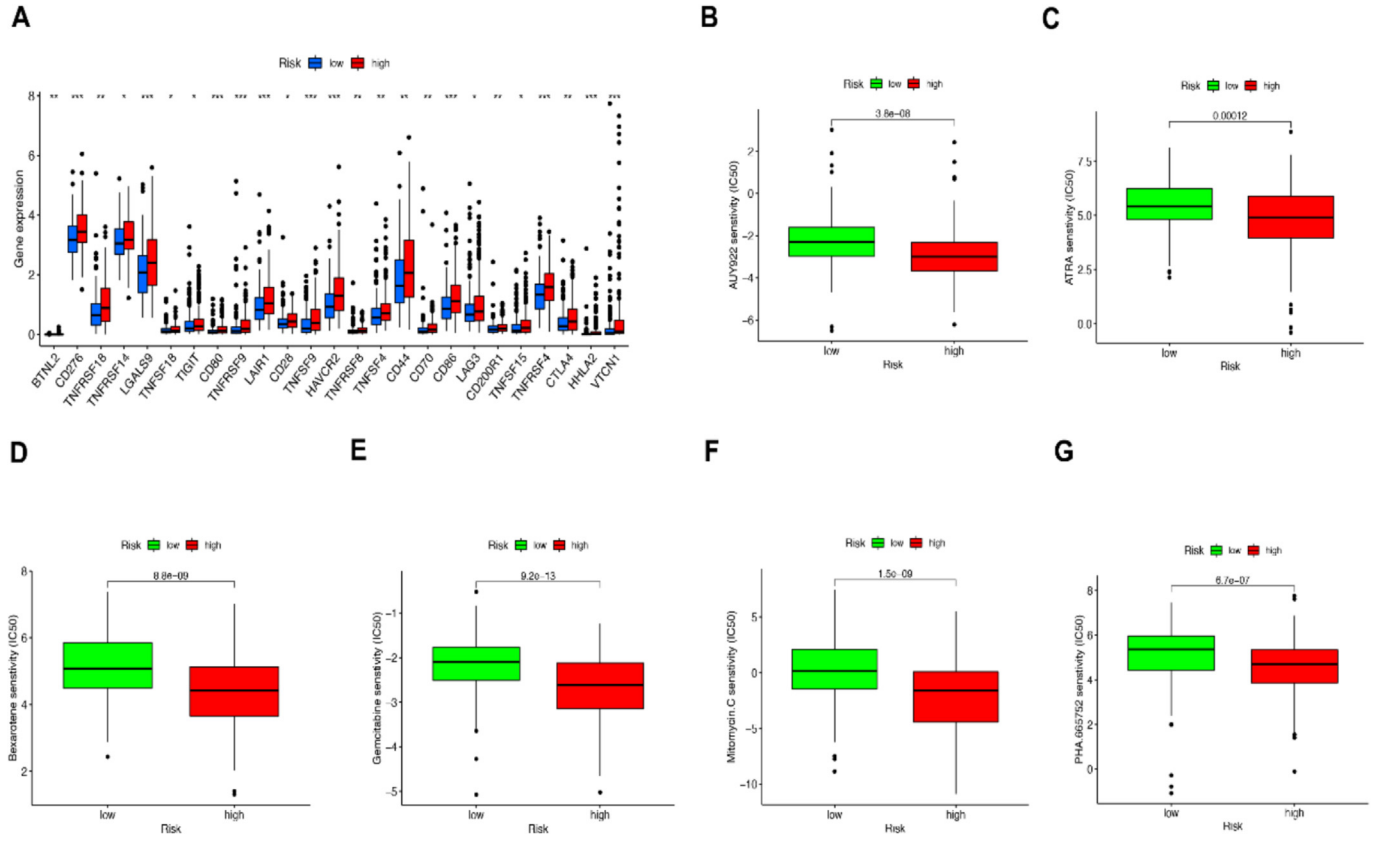

Fig. 11. Comparison of treatment drug sensitivity between high- and low-risk groups. (A) In two groups, differential expression of immune checkpoint genes in the high- and low-risk groups (Wilcox test, *$p < 0.05$; **$p < 0.01$; ***$p < 0.001$); (B–G) IC50 of AUY922, ATRA, Bexarotene, Gemcitabine, Mitomycin.C, PHA.665752 in two groups. IC50, half-maximal inhibitory concentration.

NRAV may induce Wnt/beta-catenin signaling by modulating miR-199a-3p/CISD2 axis in HCC. The potential role of AC009283.1 in proliferation and apoptosis in the HER2-enriched subtype of breast cancer was revealed by lncRNA landscape in breast cancer [56]. LINC01138 has a high frequency of HCC. The LINC01138 transcript is associated with malignant features and poor prognosis in HCC patients and is regulated by insulin-like growth factor 2 mRNA-binding proteins 1/3 (IGF2BP1/IGF2BP3). LINC01138 acts as a tumor suppressor by physically targeting PRMT5 and enhancing its protein stability by preventing ubiquitin/proteasome-mediated degradation in HCC. The discovery of LINC01138, a promising prognostic indicator, provides insight into the molecular pathogenesis of HCC and makes the LINC01138/PRMT5 axis an ideal therapeutic target for the treatment of HCC [57]. For GSEA, a group of high-risk was nourished in several biological pathways like purine metabolism signaling, pyrimidine metabolism signaling, RNA degradation and selenoamino acid metabolism. Cell cycle signaling pathway plays critical roles in influencing signal transduction and epigenetics in cancer cells [58]. The catabolism of pyrimidines and purines induces terminal differentiation towards the monocytic lineage, which regulates aberrant cell proliferation. By contrast, in particular solid tumors, the catalytic degradation of pyrimidines sustains a mesenchymal phenotype, driven by epithelial-to-mesenchymal transition [59,60]. It has recently been shown that there are systematic alterations in RNA processing in the context of cancer. It is widely found that in many cases, mutations in RNA-splicing factor genes, as well as the shortening of 3′ untranslated regions, are present.

Additionally, there is an accumulating body of evidence that other types of RNAs, like circular RNAs, can also contribute to the formation of tumors [61]. The role of seleno-amino acids, regarded as the organic forms of selenium, in regulating antioxidant defenses, enzyme activity and tumorigenesis has gained increasing recognition. Consequently, there is an increasing focus on the potential of seleno-protein-derived amino acids for a therapeutic agent in the treatment of cancers. In addition to the role in inhibiting tumor growth, there is accumulating evidence that Se-AA metabolism can alter the tumor microenvironment and enhance immunotherapy responses [62]. The GSEA outcomes were correlated with high-risk patients and tumor- and immune-related pathways. In the high-risk group, the subsequent ssGSEA results shown that B cells, activated dendritic cells, immature dendritic cells, $CD8^+$ T cells, neutrophils, NK-cells, T helper cells, plasmacytoid dendritic cells, tumor-infiltrating lymphocyte, T follicular helper cells and T regulatory cells differed significantly between the high- and low-risk groups (Fig. 9A), with lower scores. Scientific studies have demonstrated that $CD8^+$ T cells play a pivotal role in the immune response to liver-based metastasis. T cells, a critical component of the adaptive immune response, significantly affect the development of liver-based metastases. To inform future clinical treatment, it is vital to elucidate the distinct roles of the various T cell subsets [63]. In anti-tumor immunity, Natural killer (NK) and dendritic cells (DCs) are innate immune cells, which play an essential role. Natural killer cells can kill tumor cells via two distinct mechanisms: cytokine secretion and direct cytotoxicity. Dendritic cells can be crucial in initiating adaptive immune responses against tumor cells. The natural killer cells and dendritic cells are subdivided into some subsets, each endowed with a distinct set of specialized effector functions. DCs and NK cells' crosstalk resulted in activation reciprocal control, as well as immune responses' polarization. That is the result of continued exposure to non-self-circulating antigens, which give rise to immunological

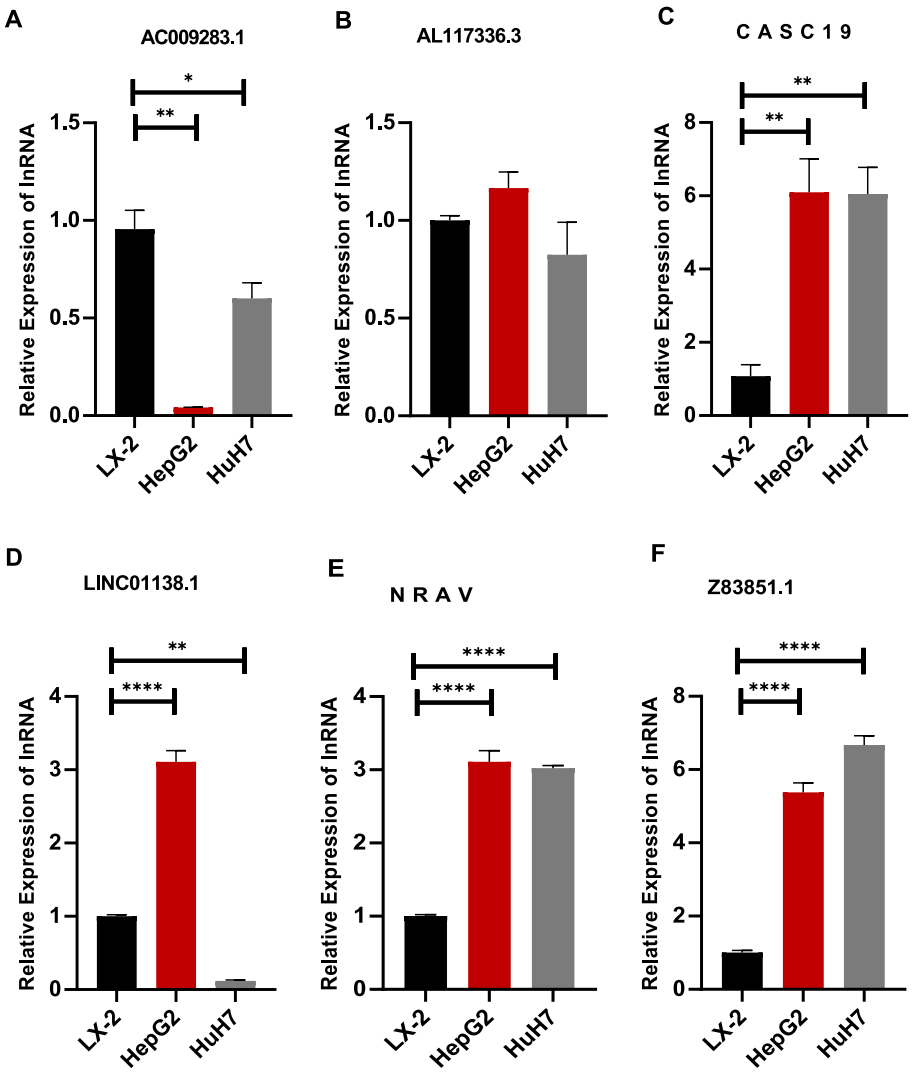

Fig. 12. The relative expression of 6 lncRNAs in different cell lines. (A–F) The relative expression of AC009283.1, AL117336.3, CASC19, LINC01138, NRAV and Z83851.1 (****$p < 0.0001$,) **$p < 0.001$, *$p < 0.05$).

features [64]. Myelopoiesis and Neutrophils can play a dual role in cancer [65]. T cells have been recognized as a vital element in leveraging the immune system's capacity to eradicate cancer cells [66]. A rise in cells of tumor-infiltrating immune and a group of the high-risk was related with a reduction in antitumor immunity, as evidenced by lower scores for several immune function scores, including those for T cell co-stimulation, checkpoint, inflammation-promoting, chemokine receptor (CCR) and Type-II-IFN-Response, as well as human leukocyte antigen (HLA). The diminished antitumor immunity observed group of high risk may be the underlying source for unfavorable prognosis.

The analysis revealed that patients classified as high risk for HCC are significantly more likely to exhibit a favorable response to several conventional chemotherapeutic agents. These include all-trans retinoic acid (ATRA), AUY922 (an HSP90 inhibitor), bexarotene (a retinoid X receptor agonist), mitomycin-C, gemcitabine, and PHA-665752 (a selective MET inhibitor). The heightened sensitivity of high-risk patients to these drugs suggests a therapeutic vulnerability that can be exploited for treatment. These findings underscore the potential of integrating molecular risk stratification into clinical decision-making, enabling the selection of chemotherapeutic agents that are more likely to be effective for specific patient subgroups. Consequently, this establishes a strong rationale for adopting a precision medicine approach in the management of HCC, where high-risk individuals could receive tailored chemotherapy regimens to improve clinical outcomes. Nevertheless, it should be noted that the research has limitations. Firstly, the TCGA database was employed exclusively for internal validation; thus, further external validation is required to ascertain the predicting signature's applicability in the broader context. TCGA samples also contained ethnic bias, and due to the retrospective design, the causality could not be inferred. In the future, an external validation cohort such as GSE14520 or ICGC-LIRI-JP should be used for model validation. Secondly, in hepatocellular carcinoma, the action' mechanism of the anoikis-related lncRNAs remains to be elucidated via further experimental verification. Future studies can also be done by looking at different methods to inhibit the progression of cancer, for example, the activation of PPARγ could possibly be an approach to induce differentiation in cells, thereby inhibiting proliferation of liver hepatocellular carcinoma, especially by inducing anoikis-mediated apoptosis [67].

5. Conclusions

To sum up, the m6A- and anoikis-related lncRNA signature is an independently validated predictor of prognosis for hepatocellular

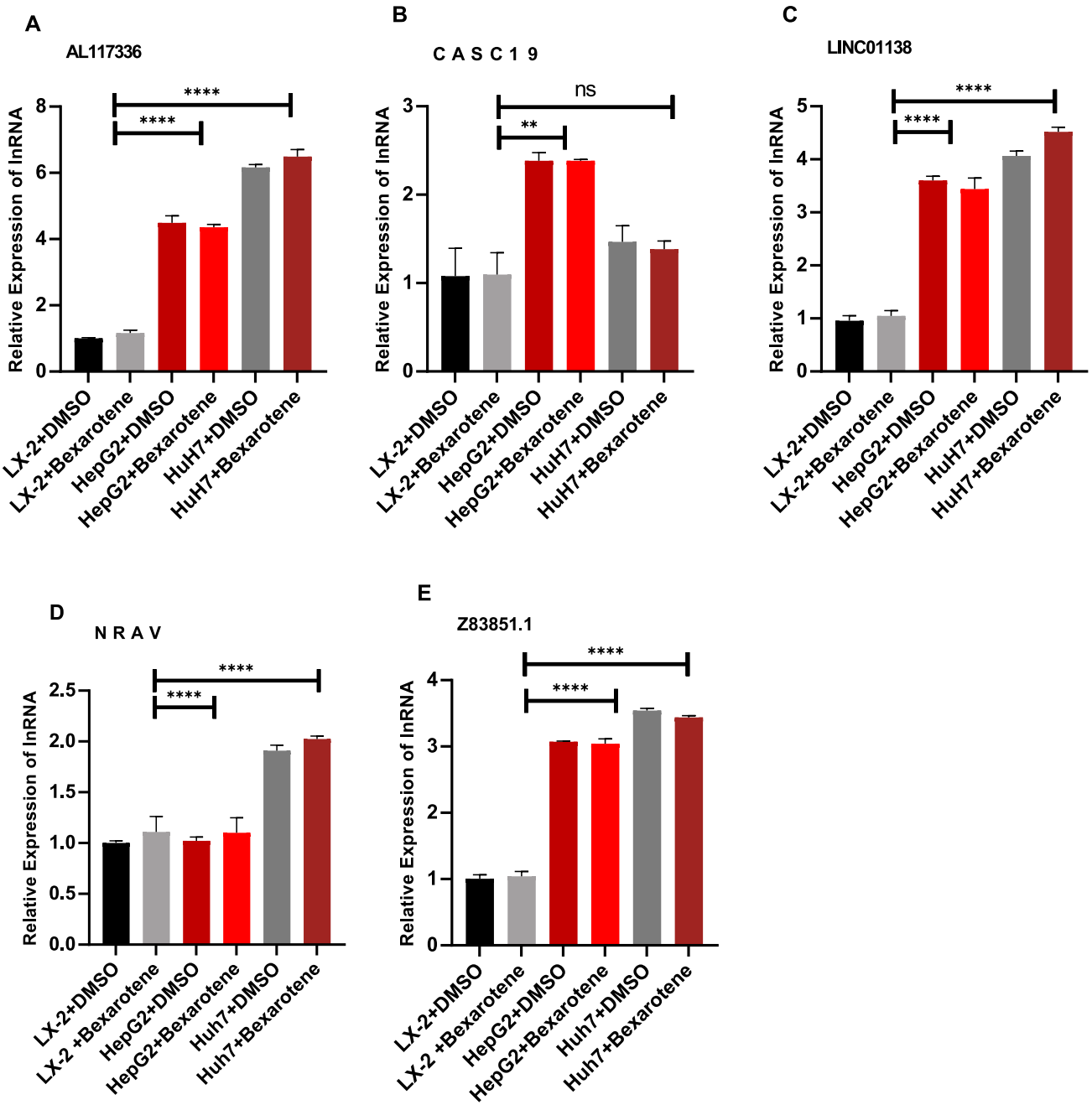

Fig. 13. The relative expression of 5 lncRNAs after treating with bexarotene in different cell lines. (A–E) The relative expression of AL117336.3, CASC19, LINC01138, NRAV and Z83851.1 (****$p < 0.0001$,) **$p < 0.001$, *$p < 0.05$, ns, non-significant, DMSO, Dimethyl sulfoxide).

carcinoma patients and provides a foundation for identifying the potential mechanisms with anoikis- and m6A-related lncRNAs in hepatocellular carcinoma and their response to clinical care. Medicine bexarotene can inhibit liver cancer cells' growth by downregulating the related lncRNAs of CASC19, LINC01138, NRAV and Z83851.1.

CRediT authorship contribution statement

Pan Yu: Writing – review & editing, Writing – original draft, Methodology, Investigation, Formal analysis. **Shuaiyang Jing:** Validation. **Sarinder Kaur Dhillon:** Writing – review & editing, Supervision.

Financial support

This research did not receive any specific grant from funding agencies in the public, commercial, or not-for-profit sectors.

Declaration of competing interests

No conflicts of interest declared by authors.

Supplementary material

https://doi.org/10.1016/j.ejbt.2025.100701.

Data availability

Data utilized in research can be obtained from the corresponding author upon reasonable demand.

References

[1] Ferlay J, Shin HR, Bray F, et al. Estimates of worldwide burden of cancer in 2008: GLOBOCAN 2008. Int J Cancer 2010;127(12):2893–917. https://doi.org/10.1002/ijc.25516. PMid: 21351269.

[2] Raza A, Sood GK. Hepatocellular carcinoma review: Current treatment, and evidence-based medicine. World J Gastroenterol 2014;20(15):4115–27. https://doi.org/10.3748/wjg.v20.i15.4115. PMid: 24764650.

[3] Kishi Y, Hasegawa K, Sugawara Y, et al. Hepatocellular carcinoma: Current management and future development-improved outcomes with surgical resection. Int J Hepatol 2011;2011(1):728103. https://doi.org/10.4061/2011/728103. PMid: 21994868.

[4] Jiang Y, Zhao X, Fu J, et al. Progress and challenges in precise treatment of tumors with PD-1/PD-L1 blockade. Front Immunol 2020;11:339. https://doi.org/10.3389/fimmu.2020.00339. PMid: 32226426.

[5] Haslam A, Prasad V. Estimation of the percentage of US patients with cancer who are eligible for and respond to checkpoint inhibitor immunotherapy drugs. JAMA Netw Open 2019;2(5):e192535. https://doi.org/10.1001/jamanetworkopen.2019.2535. PMid: 31050774.

[6] Liu JW, Supandi F, Dhillon SK. Ferroptosis-related long noncoding RNA signature predicts prognosis of clear cell renal carcinoma. Folia Biol (Praha) 2022;68(1):1–15. https://doi.org/10.14712/fb2022068010001. PMid: 36201853.

[7] Taddei ML, Giannoni E, Fiaschi T, et al. Anoikis: An emerging hallmark in health and diseases. J Pathol 2012;226(2):380–93. https://doi.org/10.1002/path.3000. PMid: 21953325.

[8] Yu Y, Liu B, Li X, et al. ATF4/CEMIP/PKCα promotes anoikis resistance by enhancing protective autophagy in prostate cancer cells. Cell Death Dis 2022;13(1):46. https://doi.org/10.1038/s41419-021-04494-x. PMid: 35013120.

[9] Shimokawa M, Yoshizumi T, Itoh S, et al. Modulation of Nqo1 activity intercepts anoikis resistance and reduces metastatic potential of hepatocellular carcinoma. Cancer Sci 2020;111(4):1228–40. https://doi.org/10.1111/cas.14320. PMid: 31968140.

[10] Michel JB. Anoikis in the cardiovascular system: Known and unknown extracellular mediators. Arterioscler Thromb Vasc Biol 2003;23(12):2146–54. https://doi.org/10.1161/01.ATV.0000099882.52647.E4. PMid: 14551156.

[11] Madajewski B, Boatman MA, Chakrabarti G, et al. Depleting tumor-NQO1 potentiates anoikis and inhibits growth of NSCLC. Mol Cancer Res 2016;14(1):14–25. https://doi.org/10.1158/1541-7786.MCR-15-0207-T. PMid: 26553038.

[12] Du S, Miao J, Zhu Z, et al. NADPH oxidase 4 regulates anoikis resistance of gastric cancer cells through the generation of reactive oxygen species and the induction of EGFR. Cell Death Dis 2018;9(10):948. https://doi.org/10.1038/s41419-018-0953-7. PMid: 30237423.

[13] Han J, Yu J, Dai Y, et al. Overexpression of miR-361-5p in triple-negative breast cancer (TNBC) inhibits migration and invasion by targeting RQCD1 and inhibiting the EGFR/PI3K/Akt pathway. Biomol Biomed 2019;19(1):52–9. https://doi.org/10.17305/bjbms.2018.3399. PMid: 29924958.

[14] Jiang X, Liu B, Nie Z, et al. The role of m6A modification in the biological functions and diseases. Signal Transduct Target Ther 2021;6(1):74. https://doi.org/10.1038/s41392-020-00450-x. PMid: 33611339.

[15] Fu Y, Dominissini D, Rechavi G, et al. Gene expression regulation mediated through reversible m^6A RNA methylation. Nat Rev Genet 2014;15(5):293–306. https://doi.org/10.1038/nrg3724. PMid: 24662220.

[16] Lan T, Li H, Zhang D, et al. KIAA1429 contributes to liver cancer progression through N6-methyladenosine-dependent post-transcriptional modification of GATA3. Mol Cancer 2019;18(1):186. https://doi.org/10.1186/s12943-019-1106-z. PMid: 31856849.

[17] Chen Y, Peng C, Chen J, et al. WTAP facilitates progression of hepatocellular carcinoma via m6A-HuR-dependent epigenetic silencing of ETS1. Mol Cancer 2019;18(1):127. https://doi.org/10.1186/s12943-019-1053-8. PMid: 31438961.

[18] Wei C, Wang B, Peng D, et al. Pan-cancer analysis shows that ALKBH5 is a potential prognostic and immunotherapeutic biomarker for multiple cancer types including gliomas. Front Immunol 2022;13:849592. https://doi.org/10.3389/fimmu.2022.849592. PMid: 35444654.

[19] Wang H, Liang L, Dong Q, et al. Long noncoding RNA miR503HG, a prognostic indicator, inhibits tumor metastasis by regulating the HNRNPA2B1/NF-κB pathway in hepatocellular carcinoma. Theranostics 2018;8(10):2814–29. https://doi.org/10.7150/thno.23012. PMid: 29774077.

[20] Schmitt AM, Chang HY. Long noncoding RNAs in cancer pathways. Cancer Cell 2016;29(4):452–63. https://doi.org/10.1016/j.ccell.2016.03.010. PMid: 27070700.

[21] Chi Y, Wang D, Wang J, et al. Long non-coding RNA in the pathogenesis of cancers. Cells 2019;8(9):1015. https://doi.org/10.3390/cells8091015. PMid: 31480503.

[22] Peng WX, Koirala P, Mo YY. LncRNA-mediated regulation of cell signaling in cancer. Oncogene 2017;36(41):5661–7. https://doi.org/10.1038/onc.2017.184. PMid: 28604750.

[23] Hou C, Wu X, Li C, et al. A cuproptosis-associated long non-coding RNA signature for the prognosis and immunotherapy of lung squamous cell carcinoma. Biomol Biomed 2023;23(4):624–33. https://doi.org/10.17305/bb.2022.8481. PMid: 36724022.

[24] Cai HJ, Zhuang ZC, Wu Y, et al. Development and validation of a ferroptosis-related lncRNAs prognosis signature in colon cancer. Biomol Biomed 2021;21(5):569–76. https://doi.org/10.17305/bjbms.2020.5617.

[25] Stelzer G, Dalah I, Stein TI, et al. *In-silico* human genomics with GeneCards. Hum Genom 2011;5(6):709. https://doi.org/10.1186/1479-7364-5-6-709. PMid: 22155609.

[26] Subramanian A, Tamayo P, Mootha VK, et al. Gene set enrichment analysis: A knowledge-based approach for interpreting genome-wide expression profiles. Proc Natl Acad Sci USA 2005;102(43):15545–50. https://doi.org/10.1073/pnas.0506580102. PMid: 16199517.

[27] Rooney MS, Shukla SA, Wu CJ, et al. Molecular and genetic properties of tumors associated with local immune cytolytic activity. Cell 2015;160(1–2):48–61. https://doi.org/10.1016/j.cell.2014.12.033. PMid: 25594174.

[28] Newman AM, Liu CL, Green MR, et al. Robust enumeration of cell subsets from tissue expression profiles. Nat Methods 2015;12(5):453–7. https://doi.org/10.1038/nmeth.3337. PMid: 25822800.

[29] Hakimi AA, Reznik E, Lee CH, et al. An integrated metabolic atlas of clear cell renal cell carcinoma. Cancer Cell 2016;29(1):104–16. https://doi.org/10.1016/j.ccell.2015.12.004. PMid: 26766592.

[30] Hugo W, Zaretsky JM, Sun L, et al. Genomic and transcriptomic features of response to anti-PD-1 therapy in metastatic melanoma. Cell 2016;165(1):35–44. https://doi.org/10.1016/j.cell.2016.02.065. PMid: 26997480.

[31] Van Allen EM, Miao D, Schilling B, et al. Genomic correlates of response to CTLA-4 blockade in metastatic melanoma. Science 2015;350(6257):207–11. https://doi.org/10.1126/science.aad0095. PMid: 26359337.

[32] Maeser D, Gruener RF, Huang RS. oncoPredict: An R package for predicting *in vivo* or cancer patient drug response and biomarkers from cell line screening data. Brief Bioinform 2021;22(6):bbab260. https://doi.org/10.1093/bib/bbab260. PMid: 34260682.

[33] Geeleher P, Cox N, Huang RS. pRRophetic: An R package for prediction of clinical chemotherapeutic response from tumor gene expression levels. PLoS One 2014;9(9):e107468. https://doi.org/10.1371/journal.pone.0107468. PMid: 25229481.

[34] Anwanwan D, Singh SK, Singh S, et al. Challenges in liver cancer and possible treatment approaches. Biochim Biophys Acta Rev Cancer 2020;1873(1):188314. https://doi.org/10.1016/j.bbcan.2019.188314. PMid: 31682895.

[35] Amini M, Looha MA, Zarean E, et al. Global pattern of trends in incidence, mortality, and mortality-to-incidence ratio rates related to liver cancer, 1990–2019: A longitudinal analysis based on the global burden of disease study. BMC Public Health 2022;22(1):604. https://doi.org/10.1186/s12889-022-12867-w. PMid: 35351047.

[36] Galicia-Moreno M, Silva-Gomez JA, Lucano-Landeros S, et al. Liver cancer: Therapeutic challenges and the importance of experimental models. Can J Gastroenterol Hepatol 2021;2021(1):8837811. https://doi.org/10.1155/2021/8837811. PMid: 33728291.

[37] Tan K, Goldstein D, Crowe P, et al. Uncovering a key to the process of metastasis in human cancers: A review of critical regulators of anoikis. J Cancer Res Clin Oncol 2013;139(11):1795–805. https://doi.org/10.1007/s00432-013-1482-5. PMid: 23912151.

[38] Chiarugi P, Giannoni E. Anoikis: A necessary death program for anchorage-dependent cells. Biochem Pharmacol 2008;76(11):1352–64. https://doi.org/10.1016/j.bcp.2008.07.023. PMid: 18708031.

[39] Cao Z, Livas T, Kyprianou N. Anoikis and EMT: Lethal "Liaisons" during cancer progression. Crit Rev Oncog 2016;21(3–4):155–68. https://doi.org/10.1615/CritRevOncog.2016016955. PMid: 27915969.

[40] Wang J, Luo Z, Lin L, et al. Anoikis-associated lung cancer metastasis: Mechanisms and therapies. Cancers 2022;14(19):4791. https://doi.org/10.3390/cancers14194791. PMid: 36230714.

[41] Du S, Cao K, Wang Z, et al. Comprehensive analysis of anoikis-related lncRNAs for predicting prognosis and response of immunotherapy in hepatocellular carcinoma. IET Syst Biol 2023;17(4):198–211. https://doi.org/10.1049/syb2.12070. PMid: 37417684.

[42] Wang WH, Hullinger RL, Andrisani OM. Hepatitis B virus X protein via the p38MAPK pathway induces E2F1 release and ATR kinase activation mediating p53 apoptosis. J Biol Chem 2008;283(37):25455–67. https://doi.org/10.1074/jbc.M801934200. PMid: 18606816.

[43] Powell E, Piwnica-Worms D, Piwnica-Worms H. Contribution of p53 to metastasis. Cancer Discov 2014;4(4):405–14. https://doi.org/10.1158/2159-8290.CD-13-0136. PMid: 24658082.

[44] Mattick JS, Amaral PP, Carninci P, et al. Long non-coding RNAs: Definitions, functions, challenges and recommendations. Nat Rev Mol Cell Biol 2023;24(6):430–47. https://doi.org/10.1038/s41580-022-00566-8. PMid: 36596869.

[45] Jiang X, Gao YL, Li JY, et al. An anoikis-related lncRNA signature is a useful tool for predicting the prognosis of patients with lung adenocarcinoma. Heliyon 2023;9(11):e22200. https://doi.org/10.1016/j.heliyon.2023.e22200. PMid: 38053861.

[46] Meng WJ, Guo JM, Huang L, et al. Anoikis-related long non-coding RNA signatures to predict prognosis and immune infiltration of gastric cancer.

Bioengineering 2024;11(9):893. https://doi.org/10.3390/bioengineering11090893. PMid: 39329635.
[47] Lu Q, Wang L, Gao Y, et al. lncRNA APOC1P1-3 promoting anoikis-resistance of breast cancer cells. Cancer Cell Int 2021;21(1):232. https://doi.org/10.1186/s12935-021-01916-w. PMid: 33902604.
[48] Qiao FH, Tu M, Liu HY. Role of MALAT1 in gynecological cancers: Pathologic and therapeutic aspects. Oncol Lett 2021;21(4):333. https://doi.org/10.3892/ol.2021.12594. PMid: 33692865.
[49] Zhang J, Li Q, Xue B, et al. MALAT1 inhibits the Wnt/β-catenin signaling pathway in colon cancer cells and affects cell proliferation and apoptosis. Biomol Biomed 2020;20(3):357–64. https://doi.org/10.17305/bjbms.2019.4408.
[50] Qu CX, Shi XC, Zai LQ, et al. LncRNA CASC19 promotes the proliferation, migration and invasion of non-small cell lung carcinoma via regulating miRNA-130b-3p. Eur Rev Med Pharmacol Sci 2019;23(3 Suppl):247–55. https://doi.org/10.26355/eurrev_201908_18654. PMid: 31389608.
[51] Wang JJ, Li XM, He L, et al. Expression and function of long non-coding RNA CASC19 in colorectal cancer. Zhongguo Yi Xue Ke Xue Yuan Xue Bao 2017;39(6):756–61. https://doi.org/10.3881/j.issn.1000-503x.2017.06.004. PMid: 29338818.
[52] Wang WJ, Guo CA, Li R, et al. Long non-coding RNA CASC19 is associated with the progression and prognosis of advanced gastric cancer. Aging 2019;11(15):5829–47. https://doi.org/10.18632/aging.102190.
[53] Wang XD, Lu J, Lin YS, et al. Functional role of long non-coding RNA CASC19/miR-140-5p/CEMIP axis in colorectal cancer progression *in vitro*. World J Gastroenterol 2019;25(14):1697–714. https://doi.org/10.3748/wjg.v25.i14.1697. PMid: 31011255.
[54] Lv J, Fan HX, Zhao XP, et al. Long non-coding RNA Unigene56159 promotes epithelial-mesenchymal transition by acting as a ceRNA of miR-140-5p in hepatocellular carcinoma cells. Cancer Lett 2016;382(2):166–75. https://doi.org/10.1016/j.canlet.2016.08.029. PMid: 27597739.
[55] Hou Y, Tang Y, Ma C, et al. Overexpression of CASC19 contributes to tumor progression and predicts poor prognosis after radical resection in hepatocellular carcinoma. Dig Liver Dis 2023;55(6):799–806. https://doi.org/10.1016/j.dld.2022.12.001. PMid: 36805849.
[56] Cedro-Tanda A, Ríos-Romero M, Romero-Córdoba S, et al. A lncRNA landscape in breast cancer reveals a potential role for AC009283.1 in proliferation and apoptosis in HER2-enriched subtype. Sci Rep 2020;10(1):13146. https://doi.org/10.1038/s41598-020-69905-z. PMid: 32753692.
[57] Li Z, Zhang J, Liu X, et al. The LINC01138 drives malignancies via activating arginine methyltransferase 5 in hepatocellular carcinoma. Nat Commun 2018;9(1):1572. https://doi.org/10.1038/s41467-018-04006-0. PMid: 29679004.
[58] You M, Xie Z, Zhang N, et al. Signaling pathways in cancer metabolism: Mechanisms and therapeutic targets. Signal Transduct Target Ther 2023;8(1):196. https://doi.org/10.1038/s41392-023-01442-3. PMid: 37164974.
[59] Yin J, Ren W, Huang X, et al. Potential Mechanisms connecting purine metabolism and cancer therapy. Front Immunol 2018;9:1697. https://doi.org/10.3389/fimmu.2018.01697. PMid: 30105018.
[60] Siddiqui A, Ceppi P. A non-proliferative role of pyrimidine metabolism in cancer. Mol Metab 2020;35:100962. https://doi.org/10.1016/j.molmet.2020.02.005. PMid: 32244187.
[61] Goodall GJ, Wickramasinghe VO. RNA in cancer. Nat Rev Cancer 2021;21(1):22–36. https://doi.org/10.1038/s41568-020-00306-0. PMid: 33082563.
[62] Liang R, Cheng A, Lu S, et al. Seleno-amino acid metabolism reshapes the tumor microenvironment: From cytotoxicity to immunotherapy. Int J Biol Sci 2024;20(7):2779–89. https://doi.org/10.7150/ijbs.95484. PMid: 38725849.
[63] Giles JR, Globig AM, Kaech SM, et al. $CD8^+$ Tcells in the cancer-immunity cycle. Immunity 2023;56(10):2231–53. https://doi.org/10.1016/j.immuni.2023.09.005. PMid: 37820583.
[64] Cazzetta V, Franzese S, Carenza C, et al. Natural killer-dendritic cell interactions in liver cancer: Implications for immunotherapy. Cancers 2021;13(9):2184. https://doi.org/10.3390/cancers13092184. PMid: 34062821.
[65] Arvanitakis K, Mitroulis I, Germanidis G. Tumor-associated neutrophils in hepatocellular carcinoma pathogenesis, prognosis, and therapy. Cancers 2021;13(12):2899. https://doi.org/10.3390/cancers13122899. PMid: 34200529.
[66] Waldman AD, Fritz JM, Lenardo MJ. A guide to cancer immunotherapy: From T cell basic science to clinical practice. Nat Rev Immunol 2020;20(11):651–68. https://doi.org/10.1038/s41577-020-0306-5. PMid: 32433532.
[67] Sakharkar MK, Shashni B, Sharma K, et al. Therapeutic implications of targeting energy metabolism in breast cancer. PPAR Res 2013;2013(1):109285. https://doi.org/10.1155/2013/109285. PMid: 23431283.